Synthesis and Conformational Analysis of Saturated 3,1,2-Benzoxazaphosphinine 2-Oxides

Henri Kivelä,[a] Zita Zalán,[a,b] Petri Tähtinen,[a] Reijo Sillanpää,[c] Ferenc Fülöp,*[b] and Kalevi Pihlaja*[a]

Keywords: Phosphorus heterocycles / Fused-ring systems / Structure elucidation / Configuration determination / Conformation analysis

N-Unsubstituted, *N*-methyl and *N*-benzyl *cis*- and *trans*-2-(hydroxymethyl)cyclohexylamines were subjected to ring closure with phenylphosphonic dichloride, phenyl dichlorophosphate and bis(2-chloroethyl)phosphoramidic dichloride in order to synthesize *P*-epimeric diastereomers of the corresponding unsubsituted and *N*-substituted 2-phenyl-, 2-phenoxy- and 2-[bis(2-chloroethyl)amino]octahydro-2*H*-3,1,2-benzoxazaphosphinine 2-oxides. The stereochemistry and conformations of the prepared compounds were analyzed mainly by variable-temperature ^{1}H, ^{13}C and ^{31}P NMR spectroscopy. Geometry optimizations were performed for some *trans*-fused molecules by utilizing the B3LYP DFT method and a locally dense basis set, followed by $J_{H,P}$ coupling constant calculations at the UB3LYP/cc-pVTZ level of theory. The population of the *N-out* conformation of the *cis*-fused compounds was found to increase with increasing steric size of the *N* substituent (H < Me < CH_2Ph), and also to be strongly influenced by the configuration at the phosphorus atom. The heteroring of the *trans*-fused compounds predominantly adopts a chair conformation with the notable exception of the (2*R**,4a*S**,8a*S**) epimers of the 2-phenoxy-substituted compounds, for which the axial tendency of OPh causes the heteroring to adopt mainly $B_{2,4a}$- and/or $^{1}S_{4a}$-type nonchair conformations.

Introduction

The synthesis and transformations of 1,3,2-oxazaphosphinane 2-oxide derivatives have been thoroughly studied in recent decades as a consequence of their potential wide-ranging synthetic applications and the therapeutic importance of this type of compounds. Alkylation and condensation reactions of *P*-benzyl-1,3,2-oxazaphosphinane 2-oxides and nucleophilic addition to vinylphosphonate derivatives that contain a 1,3,2-oxazaphosphinane ring are effective methods for the stereoselective formation of single carbon–carbon bonds.[1,2]

The 1,3,2-oxazaphosphinane ring system is found in alkylating anticancer drugs (e.g. cyclophosphamide and ifosfamide),[3] numerous derivatives of which have been synthesized in order to determine their structure–activity relationships.[4] Compounds that contain the 1,3,2-oxazaphosphinane moiety have recently been reported to possess matrix metalloproteinase-inhibitory[5] and pesticide activities.[6]

Conformational analyses of monocyclic 1,3,2-oxazaphosphinanes have revealed numerous interesting details concerning the conformational properties of the heteroring.[7] However, the synthesis and conformations of cycloalkane-condensed 1,3,2-oxazaphosphinanes have been studied less extensively. Their conformational behavior may differ from that of cycloalkane-fused 1,3-heterocycles which often adopt a biased chair–chair conformation in *trans*-fused derivatives and two interconvertible chair–chair conformations in the *cis* isomers.[8] As with bicyclic heterocycles,[8] the orientation of the substituents in the 2-position, and also the substituent on the nitrogen atom when it is next to the ring annulation position, liekly has a significant influence on the conformers that predominate.

Conformational analyses of various 2-aryloxy- and 2-bis(2-chloroethyl)amino-substituted *cis*- and *trans*-perhydro-1,3,2-benzoxazaphosphinine 2-oxides have revealed that the heteroring in these compounds can exist not only in a chair, but also in some unusual skew conformations.[9,10] The chair/skew and *O-in*/*O-out* conformational equilibria in these compounds are strongly influenced by the nature of the ring's *N* substituent.[10]

Of the regioisomeric *cis*- and *trans*-perhydro-3,1,2-benzoxazaphosphinine 2-oxides, only the 1-benzyl-2-phenyl-substituted derivatives have been reported in the literature,[11]

[a] Department of Chemistry, University of Turku,
20014 Turku, Finland
Fax: +358-2-333-6750
E-mail: kpihlaja@utu.fi
[b] Institute of Pharmaceutical Chemistry, University of Szeged,
P. O. Box 121, 6701 Szeged, Hungary
E-mail: fulop@pharma.szote.u-szeged.hu
[c] Department of Chemistry, University of Jyväskylä,
P. O. Box 35, 40351 Jyväskylä, Finland
E-mail: resillan@jyu.fi
Supporting information for this article is available on the WWW under http://www.eurjoc.org or from the author.

 DOI: 10.1002/ejoc.200400611

and their solution-state conformations have not been analyzed. As a continuation of our previous studies on cycloalkane-condensed 1,3,2-oxazaphosphinane 2-oxides,[10] the effect of *P* and *N* substituents on the stereochemistry of ring-closure reactions and the conformations of the title compounds are discussed in this paper.

Results and Discussion

Synthesis

The amino alcohols **1**–**6** were prepared according to the procedures described in the literature.[12] Compounds **1**–**6** were cyclized with phenylphosphonic dichloride, phenyl dichlorophosphate and bis(2-chloroethyl)phosphoramidic dichloride at ambient temperatures by using a procedure similar to that described earlier[10a] to give 1,4,4a,5,6,7,8,8a-octahydro-2*H*-3,1,2-benzoxazaphosphinine 2-oxides **7**–**20** (Scheme 1 and Scheme 2). In most cases, two diastereomers (**a** and **b**), which differ in their configuration at the phosphorus atom, were formed and were separated by column chromatography. The ring-closure reactions of amino alcohols **1** and **4** with phenylphosphonic dichloride proceeded with complete diastereoselectivity to give compound **7a** and **10b**, respectively, as single diastereomers; no traces of the corresponding *P* epimers (**7b** or **10a**) were detected, even in the crude products. Compound **20** was obtained as a 45:55 mixture of **20a** and **20b**. The known 1-benzyl-2-phenyl-substituted derivatives **11a**,**b** and **12a**,**b**[11] were also prepared in order to allow a comparison of the conformational effects of the different *N* substituents.

Characterization of Structures

The structures formed in the cyclization reactions were characterized by solution-state multinuclear (^{1}H, ^{13}C and ^{31}P) NMR methods and were supported by DFT calculations on compounds **8**, **10**, **14** and **16** and the X-ray crystal structure determined for **16a**. The ^{1}H and ^{13}C chemical shifts were assigned with the aid of 1D NOESY or NOE difference and 2D homonuclear (dqf-COSY) and heteronuclear (HETCOR, COLOC) correlation experiments. The proton chemical shifts and coupling constants were determined by an iterative analysis with PERCH NMR software.[13] For the *cis*-fused compounds, the ^{1}H spin systems could be solved completely, whereas the fine structure of the -$(CH_2)_4$- proton resonances of the *trans*-fused compounds was often poorly reproduced by the simulations because of the difficulties arising from overlapping signals and the complexity of the coupling network. Comprehensive NMR data are presented in the Supporting Information.

In the configurational and conformational analysis of certain 1,3,2-benzoxaza- and -dioxaphosphinine derivatives it has been possible to use the ^{31}P chemical shifts.[9,10] However, for the 2-Ph- and 2-OPh-substituted compounds studied here, the differences in δ_P between epimers were always less than ±3 ppm. Only in case of the 2-N$(CH_2CH_2Cl)_2$ derivatives were distinctive $\Delta\delta_P$ values found; epimers with

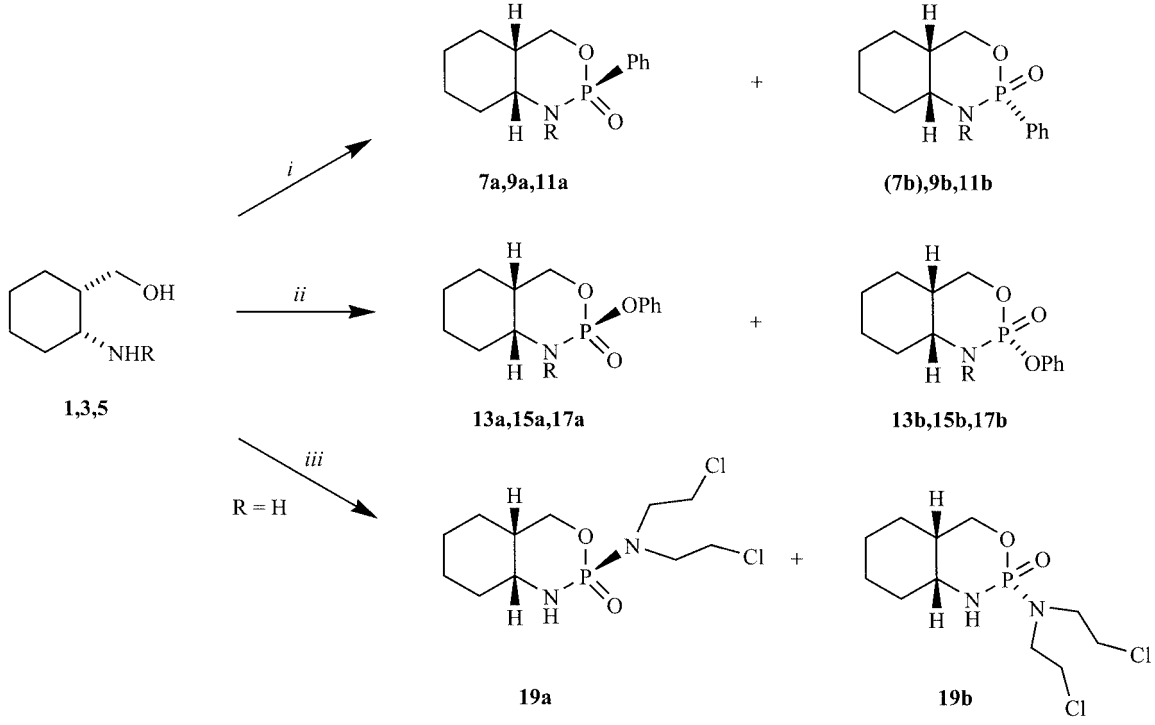

Scheme 1. Reagents: (i) Cl_2POPh/Et_3N in THF, column chromatography, 8–45%; (ii) $Cl_2PO(OPh)/Et_3N$ in THF, column chromatography, 14–37%; (iii) $Cl_2PO[N(CH_2CH_2Cl)_2]/Et_3N$ in THF, column chromatography, 30–35%. R = H: **1**, **7**, **13**; R = Me: **3**, **9**, **15**; R = CH_2Ph: **5**, **11**, **17**.

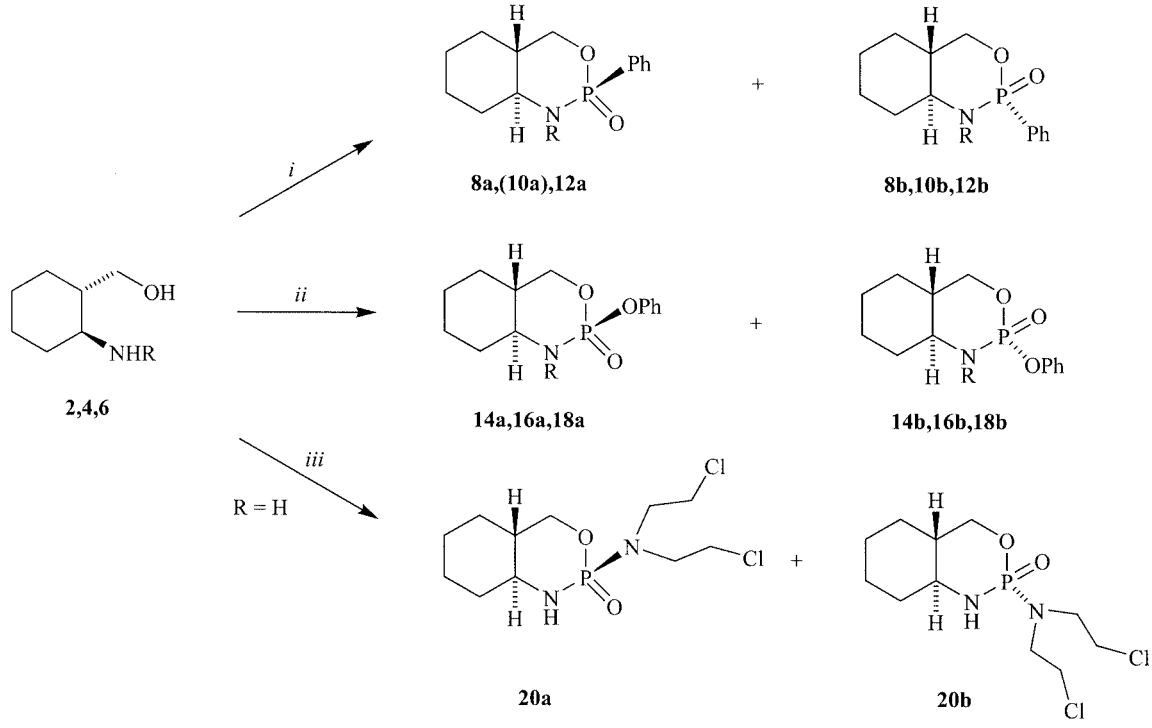

Scheme 2. Reagents: (i) Cl_2POPh/Et_3N in THF, column chromatography, 10–37%; (ii) $Cl_2PO(OPh)/Et_3N$ in THF, column chromatography, 16–42%; (iii) $Cl_2PO[N(CH_2CH_2Cl)_2]/Et_3N$ in THF, column chromatography, 63%. R = H: **2**, **8**, **14**; R = Me: **4**, **10**, **16**; R = CH_2Ph: **6**, **12**, **18**.

Table 1. Selected ^1H NMR chemical shifts [ppm] of the *trans*-fused compounds.[a]

Proton	**8a**	**8b**	**10b**	**12a**	**12b**	**14a**	**14b**	**16a**	**16b**	**18a**	**18b**	**20a**[b]	**20b**[b]
4-H_{ax}	4.22	3.64	3.79	4.12	3.81	4.07	4.07	4.06	4.03	3.93	4.08	3.87	3.77
4-H_{eq}	4.08	4.17	4.07	4.04	4.15	4.22	4.20	4.13	4.09	4.11	4.12	3.97	4.03
4a-H	1.78	1.76	2.03	1.87	2.04	1.85	1.71	2.04	1.90	2.24	1.90	1.43	1.51
8a-H	3.27	2.71	3.00	2.85	3.14	3.10	2.99	2.77	2.90	2.66	3.18	2.90	2.74

[a] In $CDCl_3$ at 25 °C, δ_{TMS} = 0.00 ppm. [b] Measured on a ca. 45:55 mixture of **20a** and **20b**; solvent $[D_6]$DMSO.

an axial P=O bond had deshielded ^{31}P resonances. This is in agreement with the results for similarly 2-substituted regioisomeric 1,3,2-benzoxazaphosphinines.[10] In this work the configurational assignments were not based on the ^{31}P chemical shifts (see the Supporting Information for δ_P values).

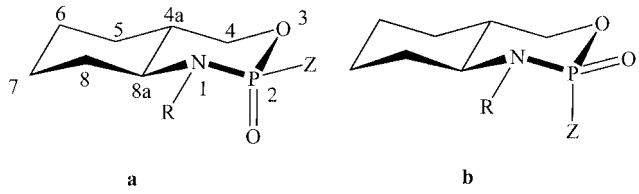

Figure 1. Diastereomers **a** and **b** of the *trans*-fused 1-R-2-Z-perhydro-3,1,2-benzoxazaphosphinine 2-oxides [R = H, Me, CH_2Ph; Z = Ph, OPh, $N(CH_2CH_2Cl)_2$]. Only chair–chair conformers are shown.

Assignment of the *P* Configuration; *trans*-Fused Compounds

The diastereomers **a** and **b** of the *P*-phenyl-substituted compounds **8**, **10** and **12** were easily identified: the 4-H_{ax} protons are deshielded (owing to the *syn*-diaxial P=O bond) with respect to the 4-H_{eq} protons in epimers **a**, whereas the opposite is true in the corresponding epimers **b** (Table 1, Figure 1). The coupling constant $^1J_{P,i\text{-}C}$ is also larger for the 2-Ph_{eq} (**a**) than for the 2-Ph_{ax} (**b**) epimers (Table 2).[14] In the *P*-bis(2-chloroethyl)amino-substituted compound **20b**, a *cis* relationship was established between 8a-H and the *P* substituent on the basis of the observed NOE in the 2-chloroethyl protons upon irradiation of 8a-H. No such NOE was observed in epimer **20a**.

In the *P*-phenoxy-substituted compounds **14**, **16** and **18**, neither NOEs nor deshielding effects on 4-H could be used to differentiate reliably between the *P* epimers. Instead, the configuration at the phosphorus atom was observed to have profound effects on the $^3J_{4\text{-}H,P}$ values. Configuration **a** was assigned to the diastereomers that had $^3J_{4\text{-}Heq,P}$ values in the range of 14–17 Hz, and **b** to those for which this coupling was approximately 24 Hz (Table 3). These differences between the diastereomeric pairs originate from the considerable differences in the preferred conformations of the

Table 2. Selected $J_{P,C}$ coupling constants [Hz] of the *trans*-fused compounds.[a]

Carbon	8a	8b	10b	12a	12b	14a	14b	16a	16b	18a	18b	20a[b]	20b[b]
C4a	4.1	6.8	6.1	7.3	5.9	11.0	5.5	11.5	4.1	12.4	3.6	3.7	7.7
C8	9.6	9.6	5.3	4.1	5.5	6.8	11.5	2.7	9.2	1.4	8.2	11.9	9.7
2-*i*-C_6H_5	180.6	165.9	162.9	182.0	164.5	7.3	7.3	7.3	9.2	6.9	8.2	–	–

[a] In $CDCl_3$ at 25 °C. [b] Measured on a ca. 45:55 mixture of **20a** and **20b**; solvent [D_6]DMSO.

Table 3. Selected $J_{H,H}$ and $J_{H,P}$ coupling constants [Hz] of the *trans*-fused compounds.[a]

Coupling	8a	8b	10b	12a	12b	14a	14b	16a	16b	18a	18b	20a[b]	20b[b]
4_{ax},4a	11.5	11.4	11.4	11.4	11.2	11.6	11.6	11.7	11.6	11.7	11.6	11.2	11.5
4_{ax},P	2.7	2.2	2.4	2.7	3.1	6.3	1.2	3.9	1.7	4.3	1.7	1.8	3.6
4_{eq},4a	4.1	4.2	4.1	3.5	4.3	4.4	4.2	3.8	4.2	3.7	4.2	4.0	4.4
4_{eq},P	20.6	21.7	21.6	19.7	21.1	14.5	23.7	16.9	24.3	15.8	24.4	22.6	19.2
4a,8a	10.3	9.9	9.9	10.7	10.1	10.6	10.1	10.6	9.9	10.8	9.9	9.9	9.1
8a,P	2.0	n.d.	n.d.	3.1	2.2	4.1	1.2	6.3	n.d.	7.3	n.d.	3.4	4.7

[a] In $CDCl_3$ at 25 °C. [b] Measured on a ca. 45:55 mixture of **20a** and **20b**; solvent [D_6]DMSO.

heteroring, as discussed below. The correct assignment of the relative *P* configuration was confirmed in the case of **16a** by X-ray crystallography (Figure 2).

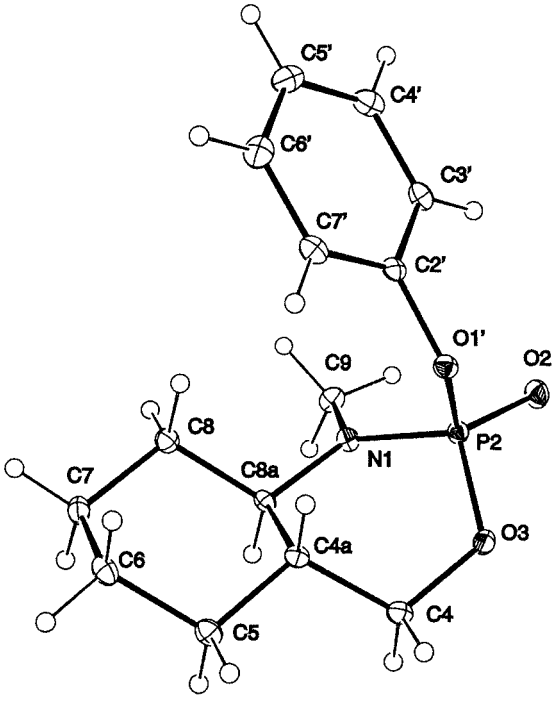

Figure 2. X-ray crystal structure of **16a**.

Assignment of the *P* Configuration; *cis*-Fused Compounds

In the *cis*-fused compounds, the possibility of ring inversion can lead to equilibria between the *N-in* and *N-out* forms (Figure 3). The equilibrium populations of these forms can be reliably deduced for each compound (vide infra, Table 7). The *P* configuration can then be inferred by comparison of the *N-in* mole fractions x(*N-in*) within each epimeric pair: the epimer in which its 2-Z substituent adopts the position preferred by the *N-in* conformation will have a larger x(*N-in*) value. Since Ph and $N(CH_2CH_2Cl)_2$ prefer an equatorial position and OPh prefers an axial position,[15] it can be concluded that the "*N-in*-favoring" epimer is **a** when Z = OPh (**13**, **15** and **17**) and **b** when Z = Ph and $N(CH_2CH_2Cl)_2$ (**9**, **11** and **19**). For **7**, only one epimer was obtained, which was assigned as **7a** on the basis of the NOE observed between the aromatic *ortho* protons and 8a-H since this enhancement is possible only in the *N-in* conformation of epimer **a** (Figure 3). For compounds **7a**, **9a**, **11a**, **11b** and **19b**, which are predominantly single invertomers, P=O-induced deshielding of one of the 4-H atoms is observed whenever P=O is axial (Table 4) thereby confirming the above diastereomeric assignments.

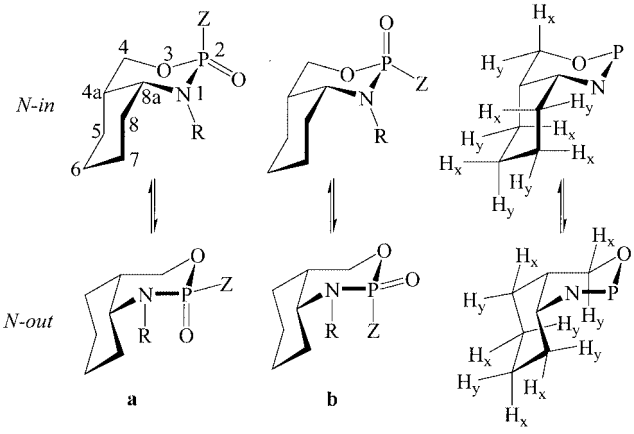

Figure 3. *N-in*/*N-out* ring inversion of epimers **a** and **b** of the *cis*-fused 1-R-2-Z-perhydro-3,1,2-benzoxazaphosphinine 2-oxides [R = H, Me, CH_2Ph; Z = Ph, OPh, $N(CH_2CH_2Cl)_2$]. Geminal protons are labeled with subscripts x and y, H_x atoms being axial in the *N-in* invertomer. Upon ring inversion, axial protons become equatorial and vice versa. Only chair–chair conformers are shown.

Table 4. Selected ^{1}H NMR chemical shifts [ppm] of the *cis*-fused compounds.[a]

Proton[b]	**7a**	**9a**	**9b**	**11a**	**11b**	**13a**	**13b**	**15a**	**15b**	**17a**	**17b**	**19a**	**19b**
4-H_x	4.06	4.04	4.49	4.06	4.30	4.49	4.22	4.37	4.09	4.31	4.10	4.16	4.53
4-H_y	4.15	4.61	4.12	4.83	4.34	4.14	4.56	4.12	4.59	4.42	4.66	4.34	3.98
4a-H	1.55	2.42	2.22	2.52	2.54	1.60	2.34	1.91	2.54	2.44	2.38	1.92	1.62
8a-H	3.54	3.21	3.43	3.01	3.07	3.77	3.44	3.42	3.08	3.28	2.98	3.48	3.87

[a] In $CDCl_3$ at 25 °C, δ_{TMS} = 0.00 ppm. [b] For the meaning of subscripts *x* and *y*, see Figure 3.

Conformations of the *trans*-Fused Compounds

Variable-temperature NMR measurements were carried out on epimers **16a** and **16b** in CD_2Cl_2, the temperature gradually being lowered to –90 °C, but no signal splitting was observed in the ^{1}H or ^{31}P NMR spectra. This is to be expected from our earlier studies on closely related structures,[10a] for which distinct heteroring conformers were observed only below 160 K in freon solutions. Such measurements, however, are plagued by experimental difficulties, such as reduced solubility at low temperatures, vanishing population of the minor conformer(s), line-broadening due to temperature instabilities and increased solvent viscosity, as well as the general difficulties involved in cooling the sample down to such low temperatures with our experimental set-up. In this work, therefore, this route was not pursued.

The *P*-Ph- and *P*-N(CH_2CH_2Cl)$_2$-substituted compounds **8**, **10**, **12** and **20** exist almost exclusively in the chair–chair conformation, regardless of the *P* configuration. This conformation is also predominant in epimers **b** of the *P*-OPh-substituted compounds (**14b**, **16b** and **18b**) since the OPh group can then occupy its preferred axial position (Figure 1). The chair conformation of the heteroring of these compounds is characterized by large values of $^3J_{4\text{-Heq,P}}$, $^3J_{4\text{-Hax,4a-H}}$ and $^3J_{4a\text{-H,8a-H}}$ (19–25, 11–12 and 9–11 Hz, respectively), and small values of $^3J_{4\text{-Hax,P}}$ and $^3J_{8a\text{-H,P}}$ (1–3.5 Hz) (Table 3), as expected from the Karplus-like dependence on the torsion angles. The values for **20b** are actually on the border of or slightly beyond these limits, suggesting that small amounts of this compound may adopt a nonchair conformation. The DFT-calculated energies (Table 5) are in good agreement with the observations for compounds in which the 2-Z substituent favors the chair conformation (**8a**, **14b** and **16b**), the lowest-energy chair–chair conformations being more than 13 kJ/mol ($\Delta G°$) more stable than the most favorable nonchair conformations of the heteroring. On the other hand, the relative energies calculated for different conformations of **8b** and **10b** predict that nonchair conformers make significant contributions to the equilibrium, which is not supported by the observed values of the coupling constants. Thus, the calculations seem to overestimate the destabilizing effect of an axial *P*-Ph group in the chair conformation. As observed recently for similar 1,3,2-benzoxazaphosphinines, the DFT calculations fail to predict the relative energies of the conformations with good accuracy at the chosen level of theory.[16] However, coupling constants are calculated with satisfactory accuracy at the selected level of theory. Indeed, in all five of the last-mentioned compounds, the calculated $J_{H,P}$ values for the optimized chair–chair conformations agree remarkably well with the observed ones. The view that no noteworthy equilibrium exists between the different heteroring conformers of compounds **14b**, **16b** and **18b** is supported by the nondependence of the above-mentioned coupling constants on the solvent or temperature (see the Supporting Information for more details).

For the epimers **14a**, **16a** and **18a**, the heteroring cannot adopt a chair conformation and the OPh group an axial position simultaneously. The anomeric effect of 2-OR in cyclophosphamide-type heterocycles is often strong enough to drive the heteroring into a skew conformation if ring inversion is restricted.[9] That is the case here. While the coupling constants $J_{4\text{-Hax,4a-H}}$, $J_{4\text{-Heq,4a-H}}$ and $J_{4a\text{-H,8a-H}}$ remain nearly the same upon changing from *P* epimer **b** to *P* epimer **a**, the $J_{H,P}$ values change significantly (Table 3). From the large values of $^3J_{4\text{-Hax,4a-H}}$ and $^3J_{4a\text{-H,8a-H}}$ and the relatively small values of $^3J_{4\text{-Hax,P}}$ and $^3J_{C8,P}$, it is evident that any nonchair conformation populated to an appreciable extent by these 2-OPh-substituted epimers **a** should lie between or close to the $B_{2,4a}$ and $^1S_{4a}$ conformations in the pseudorotational cycle depicted in Figure 4. In these conformations, the phenoxy group can occupy the preferred pseudoaxial position. The DFT-calculated geometries and energies support these conclusions; low-energy structures are predicted for compounds **14a** and **16a**, as presented in Table 5 and Figure 5. The calculations indicate that the skew conformations are relatively flexible as the conformational search for compounds **14a** and **16a** resulted in several local minimum-energy nonchair conformations within about 3.5 kJ/mol ($\Delta G°$) of each other and distributed along the above-specified sector of the pseudorotational circuit. The DFT-optimized chair–chair conformation was in both cases less stable than the most favorable chair–skew conformation by more than 5.8 kJ/mol.

The usual approach to estimating chair/skew ratios in analogous structures from fast-exchange NMR data is to assume values for the relevant $^3J_{P,H}$ coupling constants for the limiting conformers and to assign a population to each (usually two) conformer in such a way that the population-weighted average of these couplings best agrees with the observed one. Naturally, the problem is that of how to obtain these limiting values. Here, the flexibility of the nonchair conformation of the heteroring and the uncertainties in the calculated coupling constants for these conformations necessarily leave rather large margins of error in the calculated conformer populations. On the basis of the qualitative dependence of the calculated coupling constant

Table 5. $\Delta G°$ [kJ/mol] values, selected torsion angles ω [°] and $^3J_{H,P}$ coupling constants [Hz] for representative DFT-optimized conformations of compounds **8a**, **8b**, **10b**, **14a**, **14b**, **16a** and **16b**.

	Conformation[a]	$\Delta G°$	P,4-H_{ax}		P,4-H_{eq}		P,8a-H		4-H_{ax},4a-H	4-H_{eq},4a-H	P,C8
			ω	^3J	ω	^3J	ω	^3J	ω	ω	ω
8a	chair (1)	0.0	–61.7	4.2	–178.0	22.0	62.1	3.7	–179.9	–59.0	–178.7
	chair (2)	8.7	–64.6	3.4	179.4	19.8	62.1	2.8	–176.8	–56.5	179.3
	$^{3,8a}B$	15.3	–167.6	25.3	77.6	2.0	55.2	6.2	–132.3	–12.4	175.0
	$^3S_1$	37.1	–177.7	27.6	67.4	5.1	47.6	6.4	–111.2	8.4	165.0
8b	chair (2)	1.2	–69.7	2.6	174.3	21.5	71.5	0.9	179.2	–59.4	–171.3
	$^{8a}S_2$	0.0	–154.5	22.0	90.1	0.9	85.3	0.1	–154.6	–34.2	–157.1
10b	chair (1)	0.0	–64.3	3.1	179.5	22.6	83.9	–0.2	176.0	–63.3	–157.9
	chair (2)	1.4	–72.8	1.7	171.5	21.2	61.4	2.6	–174.6	–55.4	178.0
	$^3S_1$	1.6	174.2	24.5	59.0	9.0	50.9	3.4	–110.6	10.0	167.8
14a	chair (1)	7.7	–63.1	2.8	–179.4	24.2	65.3	2.0	179.4	–59.3	–175.7
	chair (2)	5.8	–64.2	2.8	179.6	23.1	63.6	2.0	–177.5	–56.8	–179.3
	$B_{2,4a}$ (1)	1.2	–101.8	3.1	142.6	14.5	106.5	4.8	178.1	–61.5	–134.3
	$B_{2,4a}$ (2)	1.5	–102.4	2.8	141.9	14.0	107.9	5.9	177.9	–61.7	–132.7
	$B_{2,4a}$ (3)	1.7	–103.5	3.1	140.8	13.4	107.4	5.6	178.5	–61.2	–133.3
	$B_{2,4a}$ (4)	2.2	–105.9	4.2	138.5	12.6	104.1	3.9	–179.9	–59.6	–136.7
	$B_{2,4a}$ (5)	0.0	–109.6	5.3	134.9	10.3	101.7	3.4	–177.7	–57.7	–139.1
	$B_{2,4a}$ (6)	3.4	–112.1	6.7	132.4	9.5	100.6	2.6	–176.7	–56.6	–140.2
14b	chair (1)	0.0	–67.9	2.8	176.0	24.8	65.9	2.6	–179.6	–58.6	–174.7
	chair (2)	2.1	–70.4	2.3	173.7	23.1	71.7	0.3	–179.3	–58.9	–171.1
	$^{8a}S_2$	16.4	–150.2	23.7	94.5	0.1	77.7	–0.2	–155.2	–34.8	–164.7
	$^{3,8a}B$	13.5	–165.3	28.4	79.5	1.7	69.4	0.9	–140.0	–19.4	–172.9
16a	chair (1)	9.0	–60.7	3.4	–177.4	24.2	69.5	1.2	178.4	–60.1	–171.9
	chair (2)	21.8	–65.6	2.8	178.2	22.3	56.7	2.8	–171.9	–51.5	173.1
	$^1S_{4a}$ (1)	0.0	–93.8	1.2	150.2	18.1	121.0	10.3	173.6	–65.4	–120.5
	$^1S_{4a}$ (2)	2.1	–93.9	1.2	150.2	18.7	119.6	8.7	174.1	–64.8	–122.2
	$^1S_{4a}$ (3)	0.4	–94.4	1.2	149.6	17.8	120.6	10.1	173.9	–65.1	–121.0
	$^1S_{4a}$ (4)	1.1	–95.5	1.4	148.5	17.3	120.1	9.5	174.5	–64.7	–121.5
16b	chair (1)	0.0	–66.8	3.1	176.9	24.2	69.5	2.3	–179.7	–58.6	–171.6
	chair (2)	8.6	–73.0	2.0	171.3	23.4	62.1	1.4	–175.5	–55.7	178.7
	$^1S_{4a}$	25.8	–87.7	–0.2	155.7	20.9	132.7	17.8	169.3	–68.5	–108.7
	$^3S_1$	24.8	178.1	29.8	63.0	6.7	55.3	4.2	–118.9	2.1	172.6

[a] See Figure 4 for crude pictorial representations of nonchair conformations: chair (1) has an equatorial *N* substituent, chair (2) an axial *N* substituent.

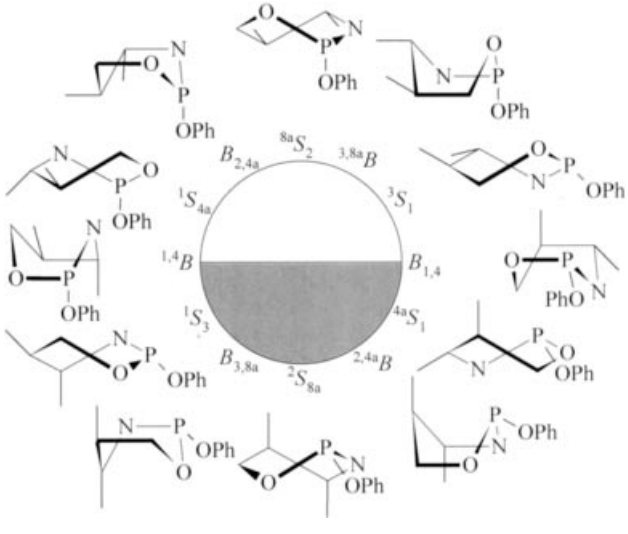

Figure 4. The idealized pseudorotational cycle for the epimers **a** of the *trans*-fused 1-R-2-OPh-perhydro-3,1,2-benzoxazaphosphinine 2-oxides. For clarity, the fused cyclohexane ring, *N* substituent and 2-oxo group have been omitted. The shaded area is inaccessible owing to conformational locking by the *trans*-fused carbocycle. The cycle is sketched for the (2*R*,4a*S*,8a*S*) enantiomers.

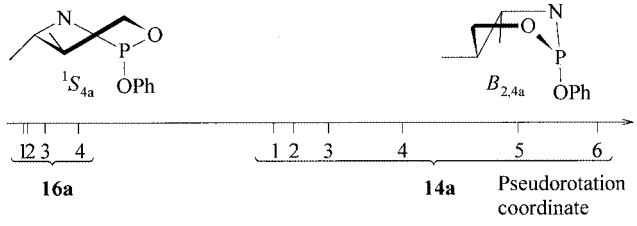

Figure 5. The nonchair conformers found for compounds **14a** and **16a** by a computational conformational search. The numbering of these conformers refers to that in Table 5. These closely related conformers arise mainly from the various rotameric states of the OPh substituent. The magnitude of the calculated torsion angle P2–O3–C4–H_{ax} was used as the pseudorotational coordinate.

$^3J_{4\text{-Hax,P}}$ on the pseudorotational coordinate (Table 5, Figure 5), it is expected that the predominant nonchair conformations of **14a** are closer to $B_{2,4a}$ than to $^1S_{4a}$ [$^3J_{4\text{-Hax,P}}$(obs) = 6.3 Hz]. By arbitrarily choosing conformation $B_{2,4a}$(6) as the model nonchair conformation for **14a**, and with the use of Equation (1), the mole fraction of the nonchair component is estimated to lie between 0.6 and 0.9. This depends on which of the two optimized chair–chair conformations is chosen as the model chair structure and which coupling constant is used ($^3J_{4\text{-Heq,P}}$ or $^3J_{4\text{-Hax,P}}$). A more precise de-

termination of this mole fraction from the time-averaged NMR data does not seem plausible owing to the above-mentioned uncertainties.

$$x(\text{nonchair}) = [J(\text{obs}) - J(\text{chair})]/[J(\text{nonchair}) - J(\text{chair})] \quad (1)$$

For **16a**, all the nonchair DFT-calculated structures found were similar to that of $^1S_{4a}$, and as such seemed to exhibit slightly too-large $^3J_{4\text{-Heq,P}}$ values (17.3–18.7 Hz vs. 16.9 Hz observed). It is therefore possible that in $CDCl_3$ the predominant nonchair conformations of **16a** are somewhat more biased towards the $B_{2,4a}$ structures than is predicted by the DFT calculations. The torsion angles measured from the X-ray crystal structure of **16a** are also consistent with this view [ω(P,4-H_{ax}) = 102.5°, ω(P,4-H_{eq}) = –141.3° (cf. Table 5)]. In any case, the $^3J_{4\text{-Heq,P}}$(obs) value together with the small value observed for $^3J_{C8,P}$ (2.7 Hz) and the intermediate $^3J_{8a\text{-H,P}}$ (6.3 Hz) suggest that the heteroring of **16a** does not populate the chair conformation in an appreciable amount (the values of $^3J_{C8,P}$ and $^3J_{8a\text{-H,P}}$ for **16b** are 9.2 and <1 Hz, respectively). This holds even more so for **18a** (1.4 and 7.3 Hz, as opposed to 8.2 and <1 Hz for **18b**). Thus, from the systematic decrease in $^3J_{C8,P}$ and the increase in $^3J_{C4a,P}$ in the sequence **14a** → **16a** → **18a**, it would be tempting to suggest that the nonchair heteroring population increases with the increasing steric size of the *N* substituent (H < Me <CH_2Ph) from perhaps 80% in **14a** to close to 100% in **18a**. Consistently with this, the DFT calculations predict an increased preference for nonchair conformations of the heteroring in **16a** as compared with **14a**. The relevant coupling constants of **14a**, **16a** and **18a** display more pronounced solvent and temperature dependencies than those of the corresponding epimers **b** (see the Supporting Information for data), which confirms that the epimers **a** exist in a conformational equilibrium whereas the epimers **b** remain exclusively in the chair–chair conformation. By assuming that the equilibrium in epimers **a** exists between the skew and chair conformers, the data show that increasing solvent polarity and temperature favor the skew heteroring over the chair.

Conformations of the *cis*-Fused Compounds

In the *cis*-fused compounds, it is expected that the fused cyclohexane moiety adopts the chair conformation. Owing to ring inversion, the heteroring's nitrogen atom can therefore be either axial (*N-in*) or equatorial (*N-out*) with respect to the cyclohexane ring (Figure 3). The equilibrium between these conformers is strongly dependent on the nature and configuration of the *P* substituents since the ring reversal permits their preferred positions to be adopted [axial for OPh, equatorial for Ph and N(CH_2CH_2Cl)$_2$] without the need for the heteroring to adopt the nonchair conformations. However, the steric size of the *N* substituent also has a marked effect on the equilibrium, as will be discussed below.

Although the interconversion between the *N-in* and *N-out* conformers is fast on the NMR timescale, resulting in time-averaged spectra at 25 °C, it is possible to estimate their equilibrium mole fractions quite accurately for the following reasons. (1) In the ring reversal process large diaxial vicinal $J_{H,H}$ couplings are exchanged for small diequatorial ones. (2) The values of these coupling constants for protons in the cyclohexane ring are relatively independent of the substitution on the heteroring. (3) Compounds **13a** and **17b** populate the *N-in* and *N-out* conformations, respectively, almost completely and hence provide reference axial–axial and equatorial–equatorial coupling constants for these conformers (Table 6). Accordingly, Equation (1), modified for the *N-in*/*N-out* equilibrium, may be utilized to calculate the equilibrium mole fractions of the ring invertomers for all of the *cis*-fused compounds **7**–**19a**,**b** (Table 7). In the following, geminal protons will be denoted as H_x or H_y according to the convention adopted in Figure 3. The *N-in* mole fractions presented in Table 7 are averages of eight calculations as there are eight suitable ^{1}H,^{1}H coupling constants in the carbocycle ($^3J_{4a\text{-H,5-Hx}}$, ... , $^3J_{8\text{-Hy,8a-H}}$ in Table 6). The mole fractions calculated from the different coupling constants are in good agreement (standard deviations <0.04), which supports the assumption that the cyclohexane moiety is always in the chair conformation. It can be seen that the preference for the *N-out* form (the *P* substituents and their configurations being kept fixed) increases with increasing steric size of the *N* substituent in the sequence H < Me < CH_2Ph. This is to be expected since in the *N-in* form the nitrogen atom is in a sterically hindered axial position with respect to the cyclohexane ring. From the x(*N-in*) values it is also evident that OPh is strongly axial-seeking, whereas the other two substituents prefer an equatorial position in the sequence Ph < N(CH_2CH_2Cl)$_2$. It can now be seen why **13a** and **17b** should stay in their sole dominant conformations assumed under point (3) above: in **13a**, both the relative configuration of the *P* substituent (OPh) and the steric size of the *N* substituent (H) favor the *N-in* conformation, whereas in **17b** these factors favor the *N-out* form (Z = OPh, R = CH_2Ph). The exclusivity of the *N-out* conformation for **17b** is supported by the observations made at low temperatures in CD_2Cl_2. In the ^{1}H NMR spectrum of **17a**, distinct signals for both conformers become visible between approximately –50 and –70 °C, with an approximate *N-in*/*N-out* ratio of 45:55 at –90 °C, whereas only a single set of signals was observed for **17b** even at –90 °C.

In order to evaluate the conformation of the heteroring in the *N-in* and *N-out* forms it is assumed that the heteroring adopts the chair conformation in the invertomer in which the *P* substituent can thus occupy its preferred position [axial for OPh; equatorial for Ph and N(CH_2CH_2Cl)$_2$]. The other ring invertomer is then expected to populate nonchair conformations. Thus, it is assumed that the heteroring adopts a chair conformation in the *N-in* forms of **9b**, **11b**, **13a**, **15a**, **17a** and **19b**, and in the *N-out* forms of **7a**, **9a**, **11a**, **13b**, **15b**, **17b** and **19a**. This assumption is supported by the observation that for the compounds that almost exclusively favor a single invertomer (**11a**, **13a**, **15b**,

Table 6. Selected $J_{H,H}$ and $J_{H,P}$ coupling constants [Hz] of the *cis*-fused compounds.[a]

Coupling[b]	7a	9a	9b	11a	11b	13a	13b	15a	15b	17a	17b	19a	19b
4_x,4a	2.7	4.0	3.3	4.5	5.0	2.5	4.0	4.0	4.2	4.8	4.4	3.6	2.8
4_x,P	4.2	16.9	7.6	20.4	13.1	1.8	18.9	2.8	22.9	7.1	23.5	12.2	2.5
4_y,4a	2.7	10.4	5.9	12.2	11.1	1.7	10.4	3.7	12.0	9.1	12.4	6.6	1.8
4_y,P	20.8	6.7	15.7	3.2	9.0	23.7	5.8	21.2	2.8	15.5	2.0	11.9	23.0
4a,5_x	11.7	3.7	8.6	2.4	3.4	12.6	4.3	10.8	2.5	5.2	2.1	7.8	12.5
5_x,6_x	12.4	4.8	9.2	2.4	4.2	13.2	4.7	11.3	3.0	5.9	2.6	8.5	13.2
5_y,6_y	4.0	12.1	7.2	14.0	12.7	3.2	12.0	5.1	13.7	10.4	14.0	8.1	3.2
6_x,7_x	12.1	4.5	9.3	2.9	3.5	13.0	4.9	11.0	3.5	6.0	3.1	8.4	13.0
6_y,7_y	3.9	11.4	7.2	13.3	12.1	3.0	11.2	4.8	12.8	10.2	13.3	7.9	3.0
7_x,8_x	12.7	5.1	9.7	3.3	3.9	13.6	5.3	11.7	3.6	6.6	3.5	9.0	13.3
7_y,8_y	3.9	11.7	7.2	13.2	12.2	3.3	11.4	5.2	12.9	10.2	13.1	7.6	4.0
8_y,8a	3.8	10.3	6.8	12.1	11.3	2.8	10.6	5.0	12.0	9.3	12.4	7.1	2.6
8_x,P	5.9	n.d.	2.1	n.d.	n.d.	7.8	n.d.	3.7	n.d.	1.7	n.d.	3.7	7.1
8a,P	2.3	14.5	3.8	20.0	12.0	1.0	20.9	3.1	22.4	8.4	22.9	11.2	1.9

[a] In $CDCl_3$ at 25 °C. [b] For the meaning of subscripts *x* and *y*, see Figure 3.

Table 7. *N-in* mole fractions and approximate values of the coupling constants $^3J_{4\text{-Hx,P}}$ and $^3J_{4\text{-Hy,P}}$ [Hz] in the limiting invertomers (*N-in* and *N-out*) of the *cis*-fused compounds. The heteroring of the invertomer A[b] is assumed to adopt the chair conformation; the coupling constants for the invertomer B[b] are back-calculated from Equation (2).

	x(*N-in*)	Δx[a]	Invertomer A[b]	^3J(obs)		^3J(*N-in*)		^3J(*N-out*)	
				4-H_x,P	4-H_y,P	4-H_x,P	4-H_y,P	4-H_x,P	4-H_y,P
7a	0.92	0.01	*N-out*	4.2	20.8	2.7	22.3	20.4[c]	3.2[c]
9a	0.17	0.03	*N-out*	16.9	6.7	0.0	23.1	20.4[c]	3.2[c]
9b	0.61	0.02	*N-in*	7.6	15.7	2.7[d]	22.3[d]	15.3	5.5
11a	0.00	0.02	*N-out*	20.4	3.2	–	–	20.4	3.2
11b	0.10	0.04	*N-in*	13.1	9.0	2.7[d]	22.3[d]	14.2	7.5
13a	1.00	–	*N-in*	1.8	23.7	1.8	23.7	–	–
13b	0.19	0.01	*N-out*	18.9	5.8	–1.0	22.1	23.5[e]	2.0[e]
15a	0.81	0.02	*N-in*	2.8	21.2	1.8[f]	23.7[f]	7.1	10.6
15b	0.03	0.01	*N-out*	22.9	2.8	4.6	26.0	23.5[e]	2.0[e]
17a	0.31	0.01	*N-in*	7.1	15.5	1.8[f]	23.7[f]	9.4	11.8
17b	0.00	–	*N-out*	23.5	2.0	–	–	23.5	2.0
19a	0.55	0.01	*N-out*	12.2	11.9	3.4	19.6	23.0[g]	2.5[g]
19b	0.99	0.03	*N-in*	2.5	23.0	2.5	23.0	–	–

[a] Standard deviation of eight calculations of x(*N-in*), each using a different coupling constant. [b] In invertomer A the *P* substituent is in a preferred position if a chair–chair conformation is adopted; B is the other invertomer. [c] From **11a**. [d] From **7a**. [e] From **17b**. [f] From **13a**. [g] From **19b**, assuming reversal of coupling constants upon ring inversion.

17b and **19b**) the heteroring is in the chair conformation, as deduced from the $^3J_{4\text{-Hx,4a-H}}$, $^3J_{4\text{-Hx,P}}$, $^3J_{4\text{-Hy,4a-H}}$, $^3J_{4\text{-Hy,P}}$ and $^3J_{8\text{a-H,P}}$ values. In these compounds, the *P* substituent is in its preferred position. By choosing suitable coupling constant model values for the *N-in* and *N-out* invertomers in which the heteroring adopts the chair conformation, it is possible to back-calculate the coupling constants for the invertomers with the "nonpreferred" *P* configuration by using Equation (2)

$$J(\mathrm{B}) = [J(\mathrm{obs}) - x(\mathrm{A}) \times J(\mathrm{A})]/x(\mathrm{B}), \quad (2)$$

where A is the ring invertomer with the preferred *P* configuration (assuming a chair conformation for the heteroring) and B the other invertomer with the nonpreferred *P* configuration. The results of the calculations are presented in Table 7. Although this approach is necessarily prone to large errors, some conclusions can be drawn. (1) In the *N-in* conformers, the heteroring always seems to populate chair-like conformations even when the *P* configuration is "unfavorable" (e.g. **7a**, **9a**, **13b** and **19a**). (2) In the *N-out* conformers, the heteroring noticeably populates nonchair conformation(s) if the *P* configuration is unfavorable (**9b**, **11b**, **15a** and **17a**). These results can be rationalized by steric factors: in the chair–chair conformation the *N-out* invertomer has its axially orientated hydrogen atoms at C4 and C6, as well as the axial *P* substituent and 8-H, facing each other, thus making the nonchair conformers more likely than in the case of the *N-in* form in which these repulsive interactions are missing. Unfortunately, the nature of these heteroring conformations and their populations can-

not be reliably assigned owing to the uncertainties in the data.

Conclusions

We have synthesized a series of *cis*- and *trans*-fused perhydro-3,1,2-benzoxazaphosphinine 2-oxides and analyzed their *P* configurations and solution-state conformations, mainly by means of NMR spectroscopy. As expected, the 2-OPh substituent strongly favors an axial position, whereas the 2-Ph and 2-$N(CH_2CH_2Cl)_2$ substituents prefer an equatorial position, the latter more so than the former. In the *trans*-fused compounds, the nonpreferred position of the 2-OPh substituent in the chair–chair conformation can cause the heteroring to predominantly populate nonchair conformations around the $B_{2,4a}$ ... $^1S_{4a}$ sector in the pseudorotational cycle. On the other hand, in the 2-Ph- and 2-$N(CH_2CH_2Cl)_2$-substituted *trans*-fused compounds, the heteroring predominantly adopts the chair conformation, regardless of the *P* configuration. In the *cis*-fused compounds, the axial or equatorial preference of the *P* substituents shifts the *N-in*/*N-out* equilibrium in a direction such that the substituents can occupy their preferred positions in the chair conformation of the heteroring. This tendency increases in the sequence Ph < $N(CH_2CH_2Cl)_2$ < OPh. The preference for the *N-out* form increases with increasing steric size of the *N* substituent (H < Me < CH_2Ph), which can result in either cooperation or competition with the above-mentioned effects of the *P* substituents. Thus, compounds **13a** and **17b**, for instance, populate almost exclusively a single invertomer (*N-in* and *N-out*, respectively), whereas in **9b** and **19a** both invertomers are noticeably populated.

Experimental Section

NMR Measurements: The ^1H, $^1H\{^{31}P\}$, $^{31}P\{^1H\}$, $^{13}C\{^1H\}$, NOE difference, dqf-COSY, CH shift correlation and COLOC NMR spectra were recorded with a JEOL JNM-LA400 (^1H: 399.78 MHz, ^{31}P: 161.84 MHz and ^{13}C: 100.54 MHz) or JEOL JNM-A500 (^1H: 500.16 MHz, ^{31}P: 202.47 MHz and ^{13}C: 125.78 MHz) instrument. Samples were typically dissolved in $CDCl_3$ and the NMR spectra were measured at 25 °C in 5-mm diameter NMR tubes. Owing to the poor solubility of compound **20** in $CDCl_3$, its NMR spectra were recorded in [D_6]DMSO at 30 °C. A few ^1H NMR experiments were also performed with [D_6]acetone as solvent (at 25 °C) in order to check solvent effects, and for low-temperature measurements (+20 to –90 °C) CD_2Cl_2 was used. ^1H and ^{13}C spectra were referenced to internal TMS (δ = 0.00 ppm), whereas in ^{31}P NMR experiments, external 90% H_3PO_4 in D_2O was used as a reference (δ = 0.00 ppm). ^1H NMR spectra were analyzed by using PERCH NMR software.[13]

Computations: The initial conformational search for compounds **8**, **10**, **14** and **16** was made at the molecular mechanics (MM+) level by using a utility implemented in the HyperChem. 7.0 molecular modeling software package. The geometries of the starting structures were optimized with *Gaussian 98*[17] utilizing the B3LYP DFT method[18] and a locally dense basis set, as follows. For the phosphorus, nitrogen and oxygen atoms, which have lone-pair electrons, the 6-31+G(d,p) basis set was applied in order to allow the orbitals to occupy a sufficiently large region of space. For the remaining atoms, the 6-31G(d,p) basis set was applied, except for the four carbon and hydrogen atoms bound to them in the outmost cyclohexane ring, which were treated with the 3-21G basis set. Vibrational analysis (1 bar, 298.15 K, scaling factor 0.9804)[19] was performed on the optimized structures to ensure that they corresponded to true energy minima and to yield the $\Delta G°$ values. Selected coupling constants $J_{H,P}$ (Fermi contact contribution only) were calculated by the finite perturbation theory (FPT) method at the spin-unrestricted UB3LYP/cc-pVTZ level by placing the perturbation on the phosphorus atom. Subsequently, the calculated couplings were scaled by using the calibration given by Equation (3). More details about the applied methods can be found in ref.[16].

$$J_{H,P} = 0.9057 \times J_{H,P}(FC) + 0.3349\ Hz \quad (3)$$

Cartesian coordinates and energies of the DFT-optimized geometries are provided as Supporting Information.

X-ray Crystallography: Suitable crystals of **16a** for X-ray measurements were grown from *n*-hexane solution. Crystal data for compound **16a** along with other experimental details are summarized in the Supporting Information. The crystallographic data were collected at 173 K on a Nonius-KappaCCD area-detector diffractometer using graphite-monochromatized Mo-K_α radiation (λ = 0.71073 Å). The data were collected by using ϕ and ω scans and processed by using *DENZO-SMN v0.93.0*.[20] The structures were solved by direct methods by using the *SHELXS-97* program[21] and full-matrix least-squares refinements on F^2 were performed by using the *SHELXL-97* program.[21] For all compounds the heavy atoms were refined anisotropically. The aromatic CH hydrogen atoms were included at fixed distances with fixed displacement parameters from their host atoms and the rest of the hydrogen atoms were refined isotropically. Figures were drawn with *Ortep-3 for Windows*.[22]

CCDC-247963 contains the supplementary crystallographic data for this paper. These data can be obtained free of charge from The Cambridge Crystallographic Data Centre via www.ccdc.cam.ac.uk/data_request/cif.

General Procedures: Melting points were recorded with a Kofler hot plate microscope apparatus and are uncorrected. Elemental analyses were performed with a Perkin–Elmer 2400 CHNS elemental analyzer. Chemicals were generally of the highest purity. For column chromatography, silica gel 60 (0.040–0.063 mm) was used. Merck Kieselgel 60F_{254} plates were used for TLC. The starting amino alcohols (**1**–**6**) were prepared according to the literature procedures.[12] Amino alcohols **1** and **2** were used for the ring-closure reactions as their hydrochlorides.

General Method for Ring-Closure Reactions: A solution of the appropriate *P*-containing reagent [phenylphosphonic dichloride, phenyl dichlorophosphate or bis(2-chloroethyl)phosphoramidic dichloride, 1 equiv.] in dry THF (50 mL) was added dropwise to a stirred solution of the appropriate amino alcohol (**1**–**6**, 6 mmol) and triethylamine (2 equiv.; 3 equiv. in the case of amino alcohol hydrochlorides **1** and **2**) in dry THF (100 mL) at room temperature . The reaction mixture was stirred for 48 h and then filtered to remove triethylamine hydrochloride. The filtrate was evaporated to dryness.

(2*S,4a*S**,8a*R**)-2-Phenyl-1,4,4a,5,6,7,8,8a-octahydro-2*H*-3,1,2-benzoxazaphosphinine 2-Oxide (7a):** The crude product (in which only the isomer **7a** was detected by ^1H NMR) was purified by col-

umn chromatography with ethyl acetate as eluent. Diastereomer **7a** (0.33 g, 22%) was crystallized by evaporation, filtered from *n*-hexane and recrystallized from diisopropyl ether/ethyl acetate: m.p. 135–137 °C. ^{1}H, ^{13}C and ^{31}P NMR spectroscopic data are given in the Supporting Information. $C_{13}H_{18}NO_2P$ (251.26): calcd. C 62.14, H 7.22, N 5.57; found: C 62.07, H 7.25, N 5.62.

(2*S,4a*S**,8a*S**)- and (2*R**,4a*S**,8a*S**)-2-Phenyl-1,4,4a,5,6,7,8,8a-octahydro-2*H*-3,1,2-benzoxazaphosphinine 2-Oxides (8a and 8b):** The crude product (in which only isomer **8b** was detected by ^{1}H and ^{31}P NMR spectroscopy, with the signals of **8a** possibly hidden beneath more intense bands) was purified by column chromatography with ethyl acetate/methanol (15:1) as eluent. The more mobile diastereomer was crystallized by evaporation and was filtered from *n*-hexane to yield isomer **8b** (0.56 g, 37%), which was recrystallized from diisopropyl ether/ethyl acetate: m.p. 149–155 °C. ^{1}H, ^{13}C and ^{31}P NMR spectroscopic data are given in the Supporting Information. $C_{13}H_{18}NO_2P$ (251.26): calcd. C 62.14, H 7.22, N 5.57; found: C 62.20, H 7.17, N 5.54.

The less mobile diastereomer was crystallized by evaporation and was filtered from *n*-hexane to yield isomer **8a** (0.15 g, 10%, m.p. 200–205 °C) with **8b** as a minor impurity (ca. 3:100 by ^{1}H NMR). ^{1}H, ^{13}C and ^{31}P NMR spectroscopic data are given in the Supporting Information. $C_{13}H_{18}NO_2P$ (251.26): calcd. C 62.14, H 7.22, N 5.57; found: C 62.08, H 7.30, N 5.63.

(2*S,4a*S**,8a*R**)- and (2*R**,4a*S**,8a*R**)-1-Methyl-2-phenyl-1,4,4a,5,6,7,8,8a-octahydro-2*H*-3,1,2-benzoxazaphosphinine 2-Oxides (9a and 9b):** The crude product (ratio of the isomers 18:82, based on the ^{31}P NMR spectrum) was purified by column chromatography with ethyl acetate/methanol (10:1) as eluent. The more mobile diastereomer was crystallized by evaporation and was filtered from *n*-hexane to yield isomer **9a** (0.21 g, 13%, m.p. 104–108 °C) in the pure form. ^{1}H, ^{13}C and ^{31}P NMR spectroscopic data are given in the Supporting Information. $C_{14}H_{20}NO_2P$ (265.29): calcd. C 63.38, H 7.60, N 5.28; found: C 63.29, H 7.57, N 5.33.

The less mobile diastereomer was crystallized by evaporation and was filtered from *n*-hexane to yield isomer **9b** (0.30 g, 19%), which was recrystallized from diisopropyl ether/ethyl acetate: m.p. 88–90 °C. ^{1}H, ^{13}C and ^{31}P NMR spectroscopic data are given in the Supporting Information. $C_{14}H_{20}NO_2P$ (265.29): calcd. C 63.38, H 7.60, N 5.28; found: C 63.41, H 7.54, N 5.30.

(2*R,4a*S**,8a*S**)-1-Methyl-2-phenyl-1,4,4a,5,6,7,8a-octahydro-2*H*-3,1,2-benzoxazaphosphinine 2-Oxide (10b):** The crude product (in which only isomer **10b** was observed by ^{1}H NMR) was purified by column chromatography with ethyl acetate/methanol (15:1) as eluent. Diastereomer **10b** (0.38 g, 24%, m.p. 58–60 °C) could be obtained by column chromatography as a pure isomer. ^{1}H, ^{13}C and ^{31}P NMR spectroscopic data are given in the Supporting Information. $C_{14}H_{20}NO_2P$ (265.29): calcd. C 63.38, H 7.60, N 5.28; found: C 63.32, H 7.63, N 5.26.

(2*S,4a*S**,8a*R**)- and (2*R**,4a*S**,8a*R**)-1-Benzyl-2-phenyl-1,4,4a,5,6,7,8,8a-octahydro-2*H*-3,1,2-benzoxazaphosphinine 2-Oxides (11a and 11b):** The crude product (ratio of the isomers 56:44, based on the ^{1}H NMR spectrum) was purified by column chromatography with ethyl acetate as eluent. The more mobile diastereomer was identified as pure isomer **11b** (0.16 g, 8%, colorless, transparent oil). ^{1}H, ^{13}C and ^{31}P NMR spectroscopic data are given in the Supporting Information. $C_{20}H_{24}NO_2P$ (341.38): calcd. C 70.37, H 7.09, N 4.10; found: C 70.47, H 7.04, N 4.14.

The less mobile diastereomer was crystallized by evaporation and was filtered from *n*-hexane to yield isomer **11a** (0.92 g, 45%), which was recrystallized from diisopropyl ether: m.p. 99–101.5 °C (lit.[11] m.p. 107–108 °C). ^{1}H, ^{13}C and ^{31}P NMR spectroscopic data are given in the Supporting Information. $C_{20}H_{24}NO_2P$ (341.38): calcd. C 70.37, H 7.09, N 4.10; found: C 70.44, H 7.13, N 4.07.

(2*S,4a*S**,8a*S**)- and (2*R**,4a*S**,8a*S**)-1-Benzyl-2-phenyl-1,4,4a,5,6,7,8,8a-octahydro-2*H*-3,1,2-benzoxazaphosphinine 2-Oxides (12a and 12b):** The crude product (ratio of the isomers 55:45, based on the ^{31}P NMR spectrum) was purified by column chromatography with ethyl acetate as eluent. The more mobile diastereomer was crystallized by evaporation and was filtered from *n*-hexane to yield isomer **12b** (0.31 g, 15%), which was recrystallized from diisopropyl ether/ethyl acetate: m.p. 145–150 °C (lit.[11] m.p. 148–149 °C). ^{1}H, ^{13}C and ^{31}P NMR spectroscopic data are given in the Supporting Information. $C_{20}H_{24}NO_2P$ (341.38): calcd. C 70.37, H 7.09, N 4.10; found: C 70.28, H 7.14, N 4.07.

The less mobile diastereomer was identified as isomer **12a** (0.37 g, 18%, colorless, transparent oil) with **12b** as a minor impurity (ca. 2:100 by ^{1}H NMR). ^{1}H, ^{13}C and ^{31}P NMR spectroscopic data are given in the Supporting Information. $C_{20}H_{24}NO_2P$ (341.38): calcd. C 70.37, H 7.09, N 4.10; found: C 70.41, H 7.06, N 4.04.

(2*R,4a*S**,8a*R**)- and (2*S**,4a*S**,8a*R**)-2-Phenoxy-1,4,4a,5,6,7,8,8a-octahydro-2*H*-3,1,2-benzoxazaphosphinine 2-Oxides (13a and 13b):** The crude product (ratio of the isomers 73:27, based on the ^{1}H NMR spectrum) was purified by column chromatography with ethyl acetate as eluent. The more mobile diastereomer was crystallized by evaporation and was filtered from diethyl ether to yield isomer **13a** (0.59 g, 37%), which was recrystallized from diisopropyl ether/ethyl acetate: m.p. 149–152 °C. ^{1}H, ^{13}C and ^{31}P NMR spectroscopic data are given in the Supporting Information. $C_{13}H_{18}NO_3P$ (267.26): calcd. C 58.42, H 6.79, N 5.24; found: C 58.50, H 6.73, N 5.27.

The less mobile diastereomer was crystallized by evaporation and was filtered from diethyl ether to yield diastereomer **13b** (0.18 g, 11%, m.p. 100–104 °C) with **13a** as a minor impurity (ca. 2:100 by ^{1}H NMR). ^{1}H, ^{13}C and ^{31}P NMR spectroscopic data are given in the Supporting Information. $C_{13}H_{18}NO_3P$ (267.26): calcd. C 58.42, H 6.79, N 5.24; found: C 58.38, H 6.83, N 5.26.

(2*R,4a*S**,8a*S**)- and (2*S**,4a*S**,8a*S**)-2-Phenoxy-1,4,4a,5,6,7,8,8a-octahydro-2*H*-3,1,2-benzoxazaphosphinine 2-oxides (14a and 14b):** The crude product (ratio of the isomers 48:52, based on the ^{31}P NMR spectrum) was purified by column chromatography with ethyl acetate as eluent. The more mobile diastereomer **14b** (0.59 g, 37%) was obtained as a crystalline compound, which was filtered from *n*-hexane and recrystallized from ethyl acetate: m.p. 160–162 °C. ^{1}H, ^{13}C and ^{31}P NMR spectroscopic data are given in the Supporting Information. $C_{13}H_{18}NO_3P$ (267.26): calcd. C 58.42, H 6.79, N 5.24; found: C 58.50, H 6.68, N 5.28.

The less mobile diastereomer **14a** (0.40 g, 25%) was crystallized by evaporation and was filtered from *n*-hexane and recrystallized from EtOAc: m.p. 103–104 °C. ^{1}H, ^{13}C and ^{31}P NMR spectroscopic data are given in the Supporting Information. $C_{13}H_{18}NO_3P$ (267.26): calcd. C 58.42, H 6.79, N 5.24; found: C 58.35, H 6.84, N 5.21.

(2*R,4a*S**,8a*R**)- and (2*S**,4a*S**,8a*R**)-1-Methyl-2-phenoxy-1,4,4a,5,6,7,8,8a-octahydro-2*H*-3,1,2-benzoxazaphosphinine 2-Oxides (15a and 15b):** The crude product (ratio of the isomers 49:51, based on the ^{1}H NMR spectrum) was purified by column chromatography with ethyl acetate as eluent. The more mobile diastereomer was identified as diastereomerically pure **15a** (0.35 g, 21%, pale yellow, transparent oil). ^{1}H, ^{13}C and ^{31}P NMR spectroscopic data are given in the Supporting Information. $C_{14}H_{20}NO_3P$

(281.29): calcd. C 59.78, H 7.17, N 4.98; found: C 59.66, H 7.20, N 4.93.

The less mobile diastereomer was identified as pure isomer **15b** (0.39 g, 23%, pale yellow, transparent oil). ^{1}H, ^{13}C and ^{31}P NMR spectroscopic data are given in the Supporting Information. $C_{14}H_{20}NO_3P$ (281.29): calcd. C 59.78, H 7.17, N 4.98; found: C 59.84, H 7.13, N 5.05.

(2*R,4a*S**,8a*S**)- and (2*S**,4a*S**,8a*S**)-1-Methyl-2-phenoxy-1,4,4a,5,6,7,8,8a-octahydro-2*H*-3,1,2-benzoxazaphosphinine 2-Oxides (16a and 16b):** The crude product (ratio of the isomers 50:50, based on the ^{31}P NMR spectrum) was purified by column chromatography with toluene/ethyl acetate (3:2) as eluent. The more mobile diastereomer was crystallized by evaporation and was filtered from *n*-hexane to yield isomer **16b** (0.62 g, 37%), which was recrystallized from *n*-hexane/diethyl ether: m.p. 101–103 °C. ^{1}H, ^{13}C and ^{31}P NMR spectroscopic data are given in the Supporting Information. $C_{14}H_{20}NO_3P$ (281.29): calcd. C 59.78, H 7.17, N 4.98; found: C 59.60, H 7.22, N 5.02.

The less mobile diastereomer was crystallized from *n*-hexane to yield isomer **16a** (0.39 g, 23%), which was recrystallized from *n*-hexane/diethyl ether: m.p. 73–74 °C. ^{1}H, ^{13}C and ^{31}P NMR spectroscopic data are given in the Supporting Information. $C_{14}H_{20}NO_3P$ (281.29): calcd. C 59.78, H 7.17, N 4.98; found: C 59.88, H 7.13, N 4.92.

(2*R,4a*S**,8a*R**)- and (2*S**,4a*S**,8a*R**)-1-Benzyl-2-phenoxy-1,4,4a,5,6,7,8,8a-octahydro-2*H*-3,1,2-benzoxazaphosphinine 2-Oxides (17a and 17b):** The crude product (ratio of the isomers 49:51, based on the ^{1}H NMR spectrum) was purified by column chromatography with *n*-hexane/ethyl acetate (2:1) as eluent. The more mobile diastereomer was identified as pure isomer **17b** (0.58 g, 27%, colorless, transparent oil). ^{1}H, ^{13}C and ^{31}P NMR spectroscopic data are given in the Supporting Information. $C_{20}H_{24}NO_3P$ (357.38): calcd. C 67.22, H 6.77, N 3.92; found: C 67.30, H 6.69, N 4.03.

The less mobile diastereomer was crystallized after evaporation and was filtered from *n*-hexane to yield the pure isomer **17a** (0.30 g, 14%, m.p. 99.5–101 °C). ^{1}H, ^{13}C and ^{31}P NMR spectroscopic data are given in the Supporting Information. $C_{20}H_{24}NO_3P$ (357.38): calcd. C 67.22, H 6.77, N 3.92; found: C 67.15, H 6.72, N 3.88.

(2*R,4a*S**,8a*S**)- and (2*S**,4a*S**,8a*S**)-1-Benzyl-2-phenoxy-1,4,4a,5,6,7,8,8a-octahydro-2*H*-3,1,2-benzoxazaphosphinine 2-Oxides (18a and 18b):** The crude product (ratio of the isomers 41:59, based on the ^{1}H NMR spectrum) was purified by column chromatography with toluene/ethyl acetate (3:2) as eluent. The more mobile diastereomer was crystallized by evaporation and was filtered from *n*-hexane to yield isomer **18b** (0.90 g, 42%), which was recrystallized from ethyl acetate: m.p. 136–139 °C. ^{1}H, ^{13}C and ^{31}P NMR spectroscopic data are given in the Supporting Information. $C_{20}H_{24}NO_3P$ (357.38): calcd. C 67.22, H 6.77, N 3.92; found: C 67.30, H 6.81, N 4.00.

The less mobile diastereomer was identified as isomer **18a** (0.34 g, 16%, colorless, transparent oil) with **18b** as a minor impurity (ca. 9:100 by ^{1}H NMR). ^{1}H, ^{13}C and ^{31}P NMR spectroscopic data are given in the Supporting Information. $C_{20}H_{24}NO_3P$ (357.38): calcd. C 67.22, H 6.77, N 3.92; found: C 67.09, H 6.72, N 3.97.

(2*R,4a*S**,8a*R**)- and (2*S**,4a*S**,8a*R**)-2-[Bis(2-chloroethyl) amino]-1,4,4a,5,6,7,8,8a-octahydro-2*H*-3,1,2-benzoxazaphosphinine 2-Oxides (19a and 19b):** The crude product (ratio of the isomers 50:50, based on the ^{31}P NMR spectrum) was purified by column chromatography with ethyl acetate/methanol (10:1) as eluent. The more mobile diastereomer was crystallized by evaporation and was filtered from *n*-hexane to yield isomer **19a** (0.66 g, 35%), which was recrystallized from diisopropyl ether/ethyl acetate: m.p. 125–127 °C. ^{1}H, ^{13}C and ^{31}P NMR spectroscopic data are given in the Supporting Information. $C_{11}H_{21}Cl_2N_2O_2P$ (315.18): calcd. C 41.92, H 6.72, N 8.89; found: C 41.81, H 6.66, N 8.93.

The less mobile diastereomer was crystallized by evaporation and was filtered from *n*-hexane to yield isomer **19b** (0.57 g, 30%), which was recrystallized from diisopropyl ether/ethyl acetate: m.p. 180–183 °C. ^{1}H, ^{13}C and ^{31}P NMR spectroscopic data are given in the Supporting Information. $C_{11}H_{21}Cl_2N_2O_2P$ (315.18): calcd. C 41.92, H 6.72, N 8.89; found: C 42.11, H 6.80, N 8.96.

(2*R,4a*S**,8a*S**)- and (2*S**,4a*S**,8a*S**)-2-[Bis(2-chloroethyl)amino]-1,4,4a,5,6,7,8,8a-octahydro-2*H*-3,1,2-benzoxazaphosphinine 2-Oxides (20a and 20b):** The crude product (ratio of the isomers 50:50, based on the ^{31}P NMR spectrum) was purified by column chromatography with ethyl acetate/methanol (7:1) as eluent. The compound was then obtained as an approximately 45:55 mixture of epimers (1.14 g, 60%). ^{1}H, ^{13}C and ^{31}P NMR spectroscopic data are given in the Supporting Information. $C_{11}H_{21}Cl_2N_2O_2P$ (315.18): calcd. C 41.92, H 6.72, N 8.89; found: C 41.79, H 6.65, N 8.94.

Supporting Information (see also footnote on the first page of this article): ^{1}H, ^{13}C and ^{31}P NMR chemical shifts, and $J_{H,H}$, $J_{H,P}$ and $J_{P,C}$ coupling constants for compounds **7**–**20a**,**b**. Solvent and temperature dependencies of coupling constants for selected *trans*-fused compounds. X-ray data for compound **16a**. Cartesian coordinates and energies of the DFT-optimized geometries.

Acknowledgments

Z. Z. is grateful for a grant from the Center for International Mobility (CIMO) in Finland. The authors thank Dr. Karel Klika for help with some NMR experiments. The Finnish IT Center for Science (CSC, Espoo, Finland) is thanked for the allocated computing time.

[1] a) S. E. Denmark, R. L. Dorow, *J. Org. Chem.* **1990**, *55*, 5926; b) S. E. Denmark, C.-T. Chen, *J. Org. Chem.* **1994**, *59*, 2922; c) N. J. Gordon, S. A. Evans, Jr., *J. Org. Chem.* **1993**, *58*, 5293; d) S. E. Denmark, J.-H. Kim, *J. Org. Chem.* **1995**, *60*, 7535.

[2] a) K. Afarinkia, H. M. Binch, E. De Pascale, *Synlett* **2000**, 1769; b) K. Afarinkia, H. M. Binch, I. Forristal, *Synlett* **2000**, 1771; c) K. Afarinkia, E. De Pascale, *Synlett* **2002**, 990; d) K. Afarinkia, E. De Pascale, S. Amara, *Arkivoc* **2002**, *6*, 205.

[3] N. Brock, *Cancer Res.* **1989**, *49*, 1.

[4] a) S. M. Ludeman, G. Zon, *J. Med. Chem.* **1975**, *18*, 1251; b) S. M. Ludeman, V. L. Boyd, J. B. Regan, K. A. Gallo, G. Zon, K. Ishii, *J. Med. Chem.* **1986**, *29*, 716; c) R. F. Borch, G. W. Canute, *J. Med. Chem.* **1991**, *34*, 3044; d) V. Gilard, R. Martino, M. Malet-Martino, B. Kutscher, A. Müller, U. Niemeyer, J. Pohl, E. E. Polymeropoulos, *J. Med. Chem.* **1994**, *37*, 3986; e) A. Paci, D. Guillaume, H.-Ph. Husson, *J. Heterocycl. Chem.* **2001**, *38*, 1131; f) A. Paci, T. Martens, J. Royer, *Bioorg. Med. Chem. Lett.* **2001**, *11*, 1347; g) L. Hu, Ch. Yu, Y. Jiang, J. Han, Zh. Li, P. Browne, P. R. Race, R. J. Knox, P. F. Searle, E. I. Hyde, *J. Med. Chem.* **2003**, *46*, 4818.

[5] Int. Patent Appl. WO 02/06293-A1; [*Chem. Abstr.* **2002**, *136*, 118577].

[6] A. E. Shipov, G. K. Genkina, O. I. Artyushin, Z. O. Mndzhoyan, B. E. Gushchin, E. I. Chumakova, S. A. Roslavtseva, O. Y. Eremina, E. I. Bakanova, Y. S. Kagan, E. A. Ershova, T. A. Mastryukova, M. I. Kabachnik, *Izv. Akad. Nauk, Ser. Khim.* **1995**, 2241 [*Chem. Abstr.* **1996**, *124*, 317319].

[7] a) G. S. Bajwa, S. Chandrasekaran, J. H. Hargis, A. E. Sopchik, D. Blatter, W. G. Bentrude, *J. Am. Chem. Soc.* **1982**, *104*, 6385; b) W. G. Bentrude, R. O. Day, J. M. Holmes, Gy. Szakal Quin, W. N. Setzer, A. E. Sopchik, R. R. Holmes, *J. Am. Chem. Soc.* **1984**, *106*, 106; c) R. R. Holmes, R. O. Day, W. N. Setzer, A. E. Sopchik, W. G. Bentrude, *J. Am. Chem. Soc.* **1984**, *106*, 2353; d) W. N. Setzer, A. E. Sopchik, W. G. Bentrude, *J. Am. Chem. Soc.* **1985**, *107*, 2083; e) W. G. Bentrude, W. N. Setzer, A. E. Sopchik, G. S. Bajwa, D. D. Burright, J. P. Hutchinson, *J. Am. Chem. Soc.* **1986**, *108*, 6669; f) W. G. Bentrude, W. N. Setzer, A. E. Sopchik, S. Chandrasekaran, M. T. Ashby, *J. Am. Chem. Soc.* **1988**, *110*, 7119; g) K. Afarinkia, R. Angell, C. L. Jones, J. Lowman, *Tetrahedron Lett.* **2001**, *42*, 743; h) S. L. Spassov, M. J. Lyapova, M. E. Ivanova, *Phosphorus Sulfur* **1988**, *37*, 199.

[8] F. Fülöp, G. Bernáth, K. Pihlaja, *Adv. Heterocycl. Chem.* **1998**, *69*, 349.

[9] a) D. G. Gorenstein, R. Rowell, *J. Am. Chem. Soc.* **1979**, *101*, 4925; b) D. G. Gorenstein, R. Rowell, J. Findlay, *J. Am. Chem. Soc.* **1980**, *102*, 5077; c) J.-C. Yang, D. O. Shah, N. U. M. Rao, W. A. Freeman, G. Sosnovsky, D. G. Gorenstein, *Tetrahedron* **1988**, *44*, 6305.

[10] a) T. Viljanen, P. Tähtinen, K. Pihlaja, F. Fülöp, *J. Org. Chem.* **1998**, *63*, 618; b) T. Viljanen, K. D. Klika, F. Fülöp, K. Pihlaja, *J. Chem. Soc., Perkin Trans. 2* **1998**, 1479.

[11] R. J. Goodridge, T. W. Hambley, D. D. Ridley, *Aust. J. Chem.* **1986**, *39*, 591.

[12] a) G. Bernáth, K. Kovács, K. L. Láng, *Acta Chim. Acad. Sci. Hung.* **1970**, *64*, 183; b) L. Gera, G. Bernáth, P. Sohár, *Acta Chim. Acad. Sci. Hung.* **1980**, *105*, 293; c) F. Fülöp, G. Bernáth, Gy. Argay, A. Kálmán, P. Sohár, *Tetrahedron* **1984**, *40*, 2053.

[13] See for example: R. Laatikainen, M. Niemitz, U. Weber, J. Sundelin, T. Hassinen, J. Vepsäläinen, *J. Magn. Reson. Ser. A* **1996**, *120*, 1; http://www.perchsolutions.com.

[14] a) G. S. Bajwa, W. G. Bentrude, *Tetrahedron Lett.* **1980**, *21*, 4683; b) W. J. Stec, W. S. Zielinski, *Tetrahedron Lett.* **1980**, *21*, 1361.

[15] W. G. Bentrude in *Phosphorus-31 NMR Spectral Properties in Compound Characterization and Structural Analysis* (Eds.: L. D. Quin, J. G. Verkade), VCH Publishers, New York, **1994**, pp. 45–46.

[16] P. Tähtinen, A. Bagno, A. Koch, K. Pihlaja, *Eur. J. Org. Chem.* **2004**, 4921.

[17] M. J. Frisch, G. W. Trucks, H. B. Schlegel, G. E. Scuseria, M. A. Robb, J. R. Cheeseman, V. G. Zakrzewski, J. A. Montgomery, Jr., R. E. Stratmann, J. C. Burant, S. Dapprich, J. M. Millam, A. D. Daniels, K. N. Kudin, M. C. Strain, O. Farkas, J. Tomasi, V. Barone, M. Cossi, R. Cammi, B. Mennucci, C. Pomelli, C. Adamo, S. Clifford, J. Ochterski, G. A. Petersson, P. Y. Ayala, Q. Cui, K. Morokuma, P. Salvador, J. J. Dannenberg, D. K. Malick, A. D. Rabuck, K. Raghavachari, J. B. Foresman, J. Cioslowski, J. V. Ortiz, A. G. Baboul, B. B. Stefanov, G. Liu, A. Liashenko, P. Piskorz, I. Komaromi, R. Gomperts, R. L. Martin, D. J. Fox, T. Keith, M. A. Al-Laham, C. Y. Peng, A. Nanayakkara, M. Challacombe, P. M. W. Gill, B. G. Johnson, W. Chen, M. W. Wong, J. L. Andres, C. Gonzalez, M. Head-Gordon, E. S. Replogle, J. A. Pople, *Gaussian 98, revision A.11*, Gaussian, Inc., Pittsburgh, PA, **2001**.

[18] a) A. D. Becke, *Phys. Rev. A* **1988**, *38*, 3098; b) A. D. Becke, *J. Chem. Phys.* **1993**, *98*, 5648; c) C. Lee, W. Yang, R. G. Parr, *Phys. Rev. B* **1988**, *37*, 785; d) B. Miehlich, A. Savin, H. Stoll, H. Preuss, *Chem. Phys. Lett.* **1989**, *157*, 200.

[19] J. B. Foresman, Æ. Frisch, *Exploring Chemistry with Electronic Structure Methods*, 2nd ed., Gaussian Inc., Pittsburgh, PA, **1996**, p. 64.

[20] Z. Otwinowski, W. Minor in *Methods in Enzymology* (Eds.: C. W. Carter, R. M. Sweet), Academic Press, London, **1997**, vol. 276, Part A, pp. 307–326.

[21] G. M. Sheldrick, *SHELXS97* and *SHELXL97*, University of Göttingen, Germany, **1997**.

[22] L. J. Farrugia, *J. Appl. Crystallogr.* **1999**, *32*, 837.

Received: August 30, 2004

